This is it!

(Submitted to Phys. Rev Letters)
March 18, 1977.

FERMILAB-PUB-77-177-E

will appear June 6, 1977

Production of the J/ψ and ψ'(3.7) by 225 GeV/c $\pi^{\pm}$ and Proton Beams on C and Sn Targets*

#6

J. G. Branson, G. H. Sanders, A. J. S. Smith, J. J. Thaler
Joseph Henry Laboratories, Princeton University,
Princeton, New Jersey 08540

and

K. J. Anderson, G. G. Henry, K. T. McDonald†,
J. E. Pilcher‡, E. I. Rosenberg
Enrico Fermi Institute, University of Chicago,
Chicago, Illinois 60637

ABSTRACT

We present results of a large acceptance experiment in which muon pairs were observed in the mass range 0.6 to 6.0 GeV/c^2. Emphasis is given to features of the production of J/ψ and ψ'(3.7) particles. We find $B\sigma(\psi'(3.7))/B\sigma(J/\psi)$ to be 0.007 ± 0.004 for p - C and 0.018 ± 0.007 for π^+- C interactions. Comparison with results from e^+e^- storage rings indicates that both the J/ψ and the ψ'(3.7) are produced strongly rather than electromagnetically in our experiment.

We have performed an experiment at Fermilab in which we observe muon pairs produced by hadron beams striking nuclear targets. This work extends our previous studies[1,2] in several ways: 1) The present exposure is 15 times the previous, some 2100 J/ψ particles having been observed; 2) the beam energy was raised to 225 GeV to map the threshold rise of J/ψ production; 3) a π^- beam was used as well as π^+ and p, allowing a search for the Drell-Yan or other electromagnetic process by comparison of π^+ with π^- induced production; 4) carbon and tin targets were used to investigate the A dependence of di-muon production.

The experiment utilized the Chicago Cyclotron Magnet Spectrometer facility described elsewhere.[1] A third threshold Cherenkov counter was added to the beamline for greater reliability in particle identification. The proportional chambers upstream of the hadron absorber[2] were not used in this analysis; the muon pairs were observed only after elimination of the hadrons. For part of the experiment low mass pairs were suppressed in the trigger by requiring a minimum separation of the muons in a scintillator hodoscope placed directly after the hadron absorber. A suppression factor of 2.2 in the trigger rate was achieved without any loss in efficiency for pairs with mass above 1.5 GeV/c^2.

For each observed pair the mass, Feynman x ($x_F = 2\ p_L^*/\sqrt{s}$), transverse momentum, and helicity angle of the μ^- in the pair rest frame are determined. A fitting procedure is used in which an assumed event vertex at the center of the target provides a constraint on the observed muon tracks, which have suffered multiple scattering in the hadron absorber. An extensive Monte Carlo simulation of the experiment is used to determine the detection efficiency as a function of the 4 kinematic variables, as well

as their experimental resolution. For masses above 1 GeV/c^2, there is negligible contamination from events originating in the absorber; in the ρ-ω mass region (0.65 - 0.95 GeV/c^2), however, a 5 - 10% contamination is present. Pairs with masses less than 0.65 GeV/c^2 will discussed in a future publication.

We calculate cross sections for directly-produced $\mu^+\mu^-$ pairs. To account for pairs due to the decay of two oppositely charged pions or kaons, we subtract the like sign pair cross sections ($\mu^+\mu^+$ and $\mu^-\mu^-$) from the raw $\mu^+\mu^-$ cross sections, assuming the like sign pairs are entirely due to meson decays.[3] Figure 1 shows the cross section for $\mu^+\mu^-$ produced in p - C interactions corrected for meson decays, as well as the observed like sign pair signal.

To display the general features of the data we group it into several mass intervals and parametrize the invariant cross section, $E\, d^3\sigma/dp^3$, by the form $A \exp(-Bp_T)\cdot(1-x_F)^C$. The results of this procedure are given in Table I, where the normalization factor A is per nucleus, integrated over the mass interval. The broad features of the x_F and p_T dependence of the data are similar to those reported in our previous work[2] as well as by others.[4,5] Discussion of the dependence on target nucleus and comparison of the non-resonant continuum production by various beams will be found in the following paper.[6] The remainder of this paper emphasizes features of J/ψ production.

Figure 2(a) illustrates the x_F dependence of J/ψ production for the π^+-, π^-- and p - C interactions, where we include all events with masses between 2.7 and 3.5 GeV/c^2 in the J/ψ signal. The pion induced distributions are flatter than the proton induced ones by a factor of approximately $(1-x_F)^{-2}$. Fits of the form $(1-x_F{}^2)^C$ yield poorer χ^2 values in all mass intervals.

From fits to $d\sigma/dx_F$ the inclusive cross section per nucleus times branching fraction for $x_F > 0$ is determined to be 120 ± 9 nb for π^--C interactions, 104 ± 12 nb for π^+-C, and 71 ± 3 nb for p-C.

Figure 2(b) shows the transverse momentum dependence of the J/ψ to be $\approx \exp(-2\ p_T)$ for all 3 beams. The data have been corrected for the systematic effect of multiple Coulomb scattering on the reconstructed value of p_T. Below p_T of 0.4 GeV/c the correction is substantial and somewhat unreliable; therefore this region has been excluded from the fits. While a fit of the form $\exp(-B\ p_T^2)$ is marginally preferable for the p_T range of our J/ψ data, it is inferior to the given fits in the lower mass regions.

In Fig. 2(c) we present helicity angle distributions for J/ψ and ρ-ω events. The J/ψ data are from all beams and both targets combined, while the ρ-ω data are from pion interactions with carbon only. We look for evidence of polarization by fitting to the form $1 + P\cos^2\theta$. For the ρ-ω data it is necessary to restrict x_F to be greater than 0.3 to obtain a broad region of useful detection efficiency, as indicated by the dashed curve in Fig. 2(c). The fitted values of the polarization parameter, P, are 0.02 ± 0.07 for the ρ-ω, and -0.28 ± 0.22 for the J/ψ. As the error on the J/ψ result is large it is useful to note that the confidence level for the hypothesis P = 0 is 35%, while for P = 1 it is 0.01%, and for P = - 1 it is 0.6%.

The energy dependence of J/ψ production is shown in Fig. 2(d), where we have extrapolated our data to $x_F = 0$ (and rapidity y = 0) to compare with other results. Linear dependence on atomic weight is used.[4,6] The increase in cross section above threshold is remarkably slow, with the invariant cross section, $d\sigma/dy$, reaching a plateau above $\sqrt{s}$ = 20 GeV.

Finally, we consider the evidence for production of the ψ'(3.7) particle. Figure 1 shows $d\sigma/dM$ for $x_F > 0.1$ in the vicinity of the J/ψ mass for the

proton beam. The solid curve is a Monte Carlo estimate of the line shape of the J/ψ . After subtracting the tail of the J/ψ in the mass region 2 - 2.7 GeV/c^2 we obtain the dashed curve with $1/M^{6.2}$ behavior as the estimate of the μ-pair continuum in the region 2 - 4 GeV/c^2. This estimate extrapolates well towards our one high mass datum point at 4.7 GeV/c^2. A significant signal remains above both this continuum[7] and the high mass tail of the J/ψ near the mass 3.7 GeV/c^2. Subtracting both effects we obtain the ratios of branching fraction times cross section for production with $x_F > 0.1$:

$$\frac{B\sigma(\psi'(3.7))}{B\sigma(J/\psi)} = 0.007 \pm 0.004 \quad (p\text{-}C)$$

$$= 0.018 \pm 0.007 \quad (\pi^+\text{-}C)$$

Due to the higher level of the μ-pair continuum in π^--C interactions it is difficult to evaluate this ratio which appears, if anything, larger. Our result for proton beams is somewhat smaller than a previous result[5] at 400 GeV beam energy and $x_F = 0$, which may, however, be due to different energy dependence of the cross sections of the J/ψ and ψ'(3.7).

Although the ψ'(3.7) appears to be much less copiously produced than the J/ψ we may still conclude it is produced by a strong interaction rather than an intermediate virtual photon by the following argument. As an extreme we suppose all of the continuum production of muon pairs shown in Fig. 1 is due to an electromagnetic interaction, such as the Drell-Yan[8] process. Then we may compare our ratios of resonance to continuum production (integrated over a suitable interval) to those obtained from J/ψ and ψ'(3.7) production at SPEAR.[9,10] For the J/ψ our resonance/continuum signal is 80 times stronger than that at SPEAR, while for the ψ'(3.7) it

is 15 times stronger. This analysis, which includes the effects of branching fraction and cross section mass dependence, thus indicates that both the J/ψ and $\psi'(3.7)$ are hadronically produced in our experiment.

This observation, as well as the flatter x_F distributions for pion induced J/ψ events compared to proton induced, is in agreement with gluon fusion models[11,12] in which the J/ψ and $\psi'(3.7)$ come principally from decays of even-charge-conjugation χ states, rather than from direct production. The absence of charmed particle production in association with the J/ψ events[4,16] also supports the gluon fusion picture.

We are pleased to note our continuing indebtedness to the staff of the Fermilab Neutrino Division, and to the members of the Chicago-Harvard-Illinois-Oxford collaboration. We have been greatly assisted in the data analysis by G. E. Hogan and C. Newman.

REFERENCES

* Work supported in part by the U. S. Energy Research and Development Administration and by the National Science Foundation. The experiment was performed at the Fermilab.

† Enrico Fermi Postdoctoral Fellow, present address: Joseph Henry Laboratories, Princeton University, Princeton, New Jersey 08540.

‡ Alfred P. Sloan Foundation Fellow.

1. K. J. Anderson, et al., Phys. Rev. Lett. 36, 237 (1976).
2. K. J. Anderson, et al., Phys. Rev. Lett. 37, 799 (1976).
3. While two particle correlations for opposite sign pion pairs are 1.5 times those of like sign pairs at 0.5 GeV/c^2 mass, they are essentially equal above 1.0 GeV/c^2 mass. See F. C. Winkelmann et al., Phys. Lett. 56B, 101 (1975).
4. M. Binkley, et al., Phys. Rev. Lett. 37, 571, 574, 578 (1976).
5. H. D. Snyder, et al., Phys. Rev. Lett. 36, 1415 (1976).
6. J. G. Branson, et al., following paper.
7. The continuum signal may also be estimated from the data of D. C. Hom et al., Phys. Rev. Lett. 37, 1374 (1976) and L. Kluberg et al., Phys. Rev. Lett. 37, 1451 (1976) under the assumption of Drell-Yan scaling. This leads to a lower estimate of the continuum than shown in Fig. 1 (see also Fig. 1 of Ref. 6) and hence a ratio of 0.009 ± 0.004 for $B\sigma$ of the ψ' compared to the J/ψ particle for p-C interactions.
8. Sidney D. Drell and Tung-Mow Yan, Phys. Rev. Lett. 25, 316 (1970).
9. A. M. Boyarski et al., Phys. Rev. Lett. 34, 1357 (1975).
10. V. Luth et al., Phys. Rev. Lett. 35, 1124 (1975).
11. S. D. Ellis, et al., Phys. Rev. Lett. 36, 1263 (1976).
12. C. E. Carlson and R. Suaya, Phys. Rev. D14, 3115 (1976).

References (continued)

13. J. J. Aubert, et al., Phys. Rev. Lett. 33, 1404 (1974).

14. Y. M. Antipov, et al., Phys. Letters 60B, 309 (1976).

15. F. W. Büsser, et al., Phys. Letters 56B, 482 (1975).

16. J. G. Branson, et al., Phys. Rev. Lett. (to be published March 14).

TABLE CAPTION

1. Results of fits of the invariant cross section, $E\, d^3\sigma/dp^3$, to the form $A \exp(-Bp_T)(1-x_F)^C$ in seven mass intervals for each of the various beam and target combinations. The normalization is per nucleus, integrated over the mass interval.

TABLE I

TARGET	MASS INTERVAL (GeV/c^2)	π^+ BEAM A $nb/GeV^2/c^3$	π^+ BEAM B $(GeV/c)^{-1}$	π^+ BEAM C	π^- BEAM A $nb/GeV^2/c^3$	π^- BEAM B $(GeV/c)^{-1}$	π^- BEAM C	PROTON BEAM A $nb/GeV^2/c^3$	PROTON BEAM B $(GeV/c)^{-1}$	PROTON BEAM C
C	0.65 - 0.95	$8.81 \pm .36 \times 10^3$	$3.87 \pm .06$	$1.35 \pm .08$	$7.45 \pm .33 \times 10^3$	$3.81 \pm .05$	$.92 \pm .07$	$1.14 \pm .04 \times 10^4$	$3.64 \pm .06$	$3.14 \pm .08$
	0.95 - 1.1	$1.26 \pm .09 \times 10^3$	$3.57 \pm .07$	$1.67 \pm .17$	$1.09 \pm .09 \times 10^3$	$3.51 \pm .09$	$1.60 \pm .16$	$1.55 \pm .09 \times 10^3$	$3.39 \pm .06$	$3.82 \pm .14$
	1.1 - 1.5	690 ± 100	$3.39 \pm .09$	$2.30 \pm .33$	469 ± 67	$3.14 \pm .09$	$1.81 \pm .33$	820 ± 84	$3.19 \pm .09$	$4.26 \pm .29$
	1.5 - 1.9	130 ± 28	$3.19 \pm .21$	$2.17 \pm .41$	87 ± 18	$2.88 \pm .21$	$2.04 \pm .33$	109 ± 15	$2.65 \pm .11$	$4.09 \pm .33$
	1.9 - 2.3	8.1 ± 7.2	$2.17 \pm .93$	$.80 \pm .44$	13.1 ± 6.0	$2.38 \pm .42$	$1.28 \pm .59$	29.3 ± 6.8	$2.71 \pm .20$	$3.25 \pm .47$
	2.3 - 2.7	4.3 ± 2.6	$2.10 \pm .50$	$.75 \pm .67$	8.1 ± 4.4	$2.15 \pm .35$	$1.06 \pm .75$	10.4 ± 3.3	$2.02 \pm .23$	$3.89 \pm .61$
	2.7 - 3.5	84.8 ± 15.0	$2.06 \pm .10$	$1.33 \pm .21$	102 ± 19	$1.98 \pm .13$	$1.93 \pm .20$	89.8 ± 9.5	$2.05 \pm .09$	$3.44 \pm .14$
Sn	0.65 - 0.95	$4.95 \pm .38 \times 10^4$	$3.44 \pm .08$	$2.23 \pm .18$				$6.58 \pm .51 \times 10^4$	$3.28 \pm .07$	$4.47 \pm .20$
	0.95 - 1.1	$7.51 \pm .79 \times 10^3$	$3.19 \pm .11$	$2.16 \pm .24$				$9.57 \pm .89 \times 10^3$	$3.11 \pm .07$	$4.76 \pm .21$
	1.1 - 1.5	$5.70 \pm 1.04 \times 10^3$	$3.36 \pm .14$	$2.71 \pm .48$				$6.58 \pm .68 \times 10^3$	$3.11 \pm .09$	$5.39 \pm .31$
	1.5 - 1.9	475 ± 100	$2.61 \pm .27$	$2.05 \pm .92$				$1.19 \pm .24 \times 10^3$	$3.20 \pm .18$	$4.28 \pm .53$
	1.9 - 2.3	59 ± 51	$1.36 \pm .48$	2.30 ± 1.30				219 ± 83	$2.42 \pm .29$	$3.59 \pm .80$
	2.3 - 2.7	160 ± 166	$1.78 \pm .76$	4.24 ± 1.88				47 ± 29	$2.22 \pm .35$	2.53 ± 1.21
	2.7 - 3.5	513 ± 118	$1.78 \pm .15$	$1.50 \pm .28$				776 ± 161	$2.02 \pm .14$	$4.01 \pm .37$

FIGURE CAPTIONS

Fig. 1 Distribution of $d\sigma/dM$ for $x_F > 0.1$ for p-carbon interactions. The solid points are $\mu^+\mu^-$ data corrected for π and K decay and the open points are $\mu^+\mu^+$ and $\mu^-\mu^-$ data combined. The solid curves are Monte Carlo estimates of the line shapes of the J/ψ and $\psi'(3.7)$. The dashed curve is an estimate of the muon pair continuum in the mass region 2-2.7 GeV/c^2, extrapolated to higher masses. A small shoulder near 3.7 GeV/c^2 is the $\psi'(3.7)$ signal.

Fig. 2 (a) Distribution of $E\, d\sigma/dx_F$ for the mass interval 2.7 - 3.5 GeV/c^2, for production of muon pairs in π^+, π^- and proton interactions with carbon. The solid lines are fits (see text).

(b) Distribution of $E/p_T\, d\sigma/dp_T$ for the same data as in (a). We require $x_F > 0.1$. The data plotted with triangles were not used in the fits (see text).

(c) Distributions of $d\sigma/d\cos\theta$, where θ is the helicity angle of the μ^- in the pair rest frame, for events with masses in the ranges 0.65 - 0.95 and 2.7 - 3.5 GeV/c^2. The solid lines are fits (see text), while the dashed lines are the detection efficiencies.

(d) Energy dependence of J/ψ production at 90° in the C.M. frame, plotted for 2 forms of the cross section. The curves are only to guide the eye.

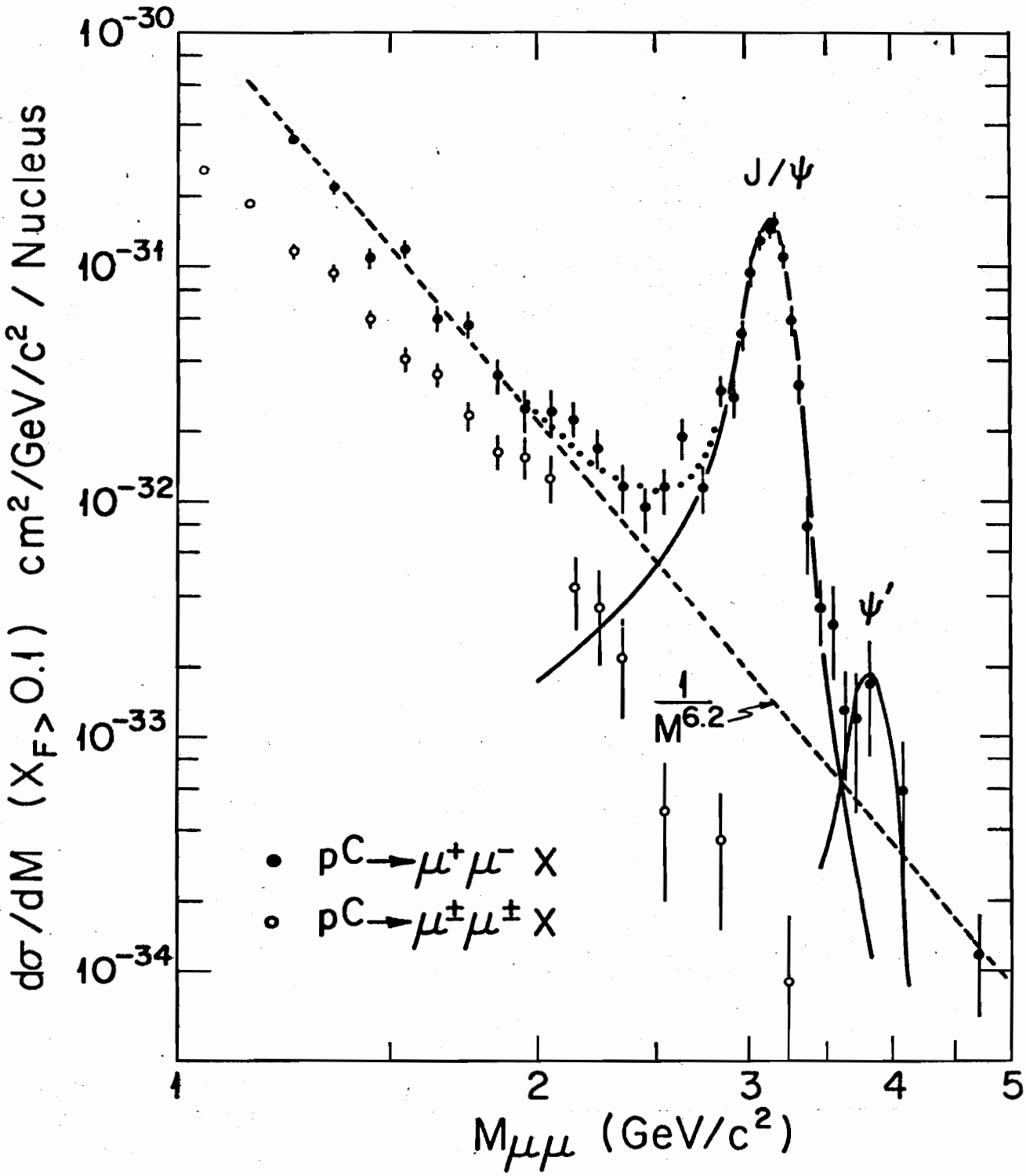
10^{-30}
10^{-31}
10^{-32}
10^{-33}
10^{-34}
$d\sigma/dM$ $(X_F > 0.1)$ $cm^2/GeV/c^2$ / Nucleus
J/ψ
ψ'
$\frac{1}{M^{6.2}}$
• $pC \rightarrow \mu^+\mu^- X$
○ $pC \rightarrow \mu^\pm\mu^\pm X$
1
2
3
4
5
$M\mu\mu$ (GeV/c^2)

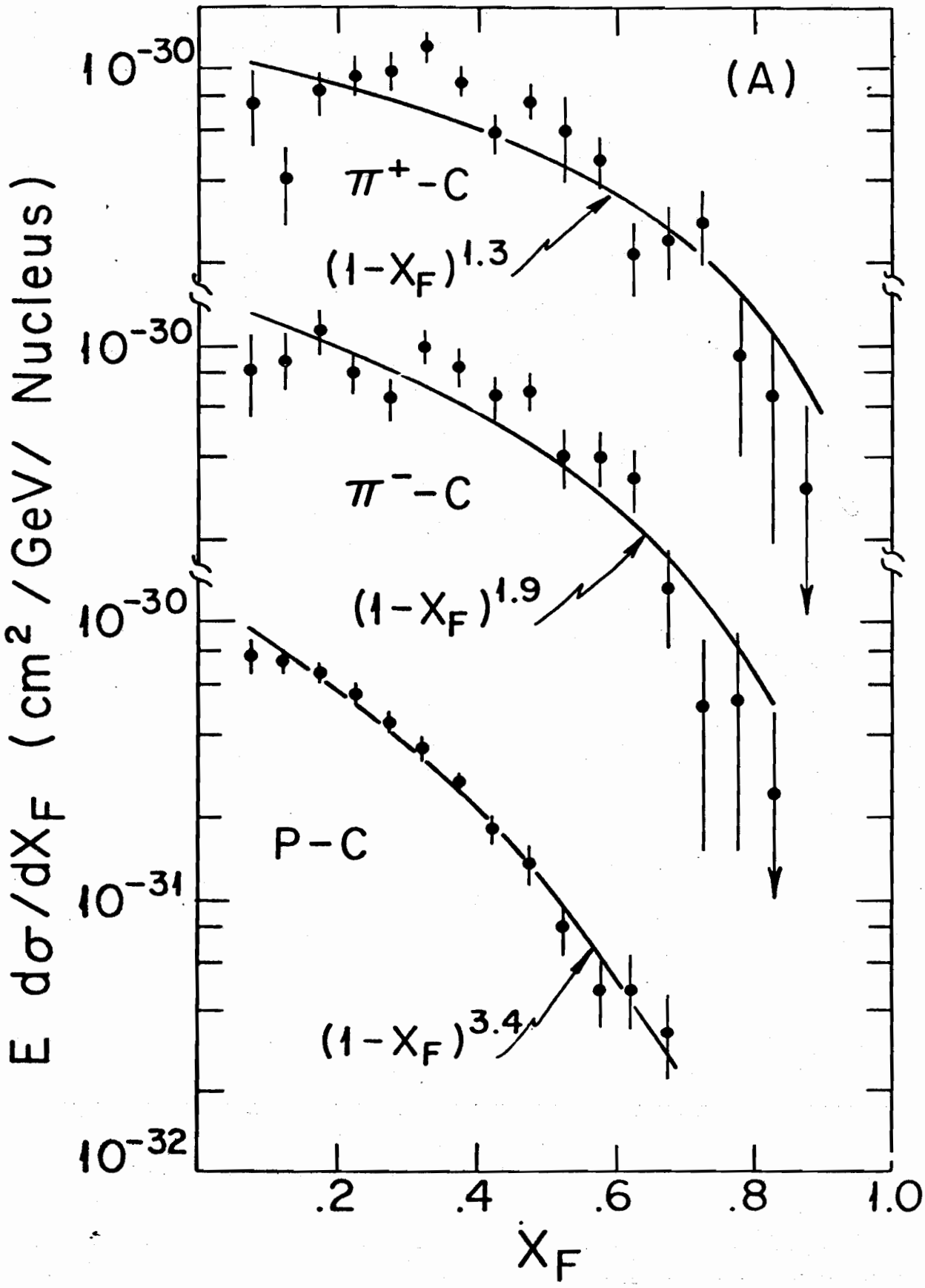
(A)
10^{-30}
10^{-30}
10^{-30}
10^{-31}
10^{-32}
$\pi^+ - C$
$(1-X_F)^{1.3}$
$\pi^- - C$
$(1-X_F)^{1.9}$
P-C
$(1-X_F)^{3.4}$
E $d\sigma/dX_F$ (cm^2 / GeV/ Nucleus)
.2
.4
.6
.8
1.0
X_F

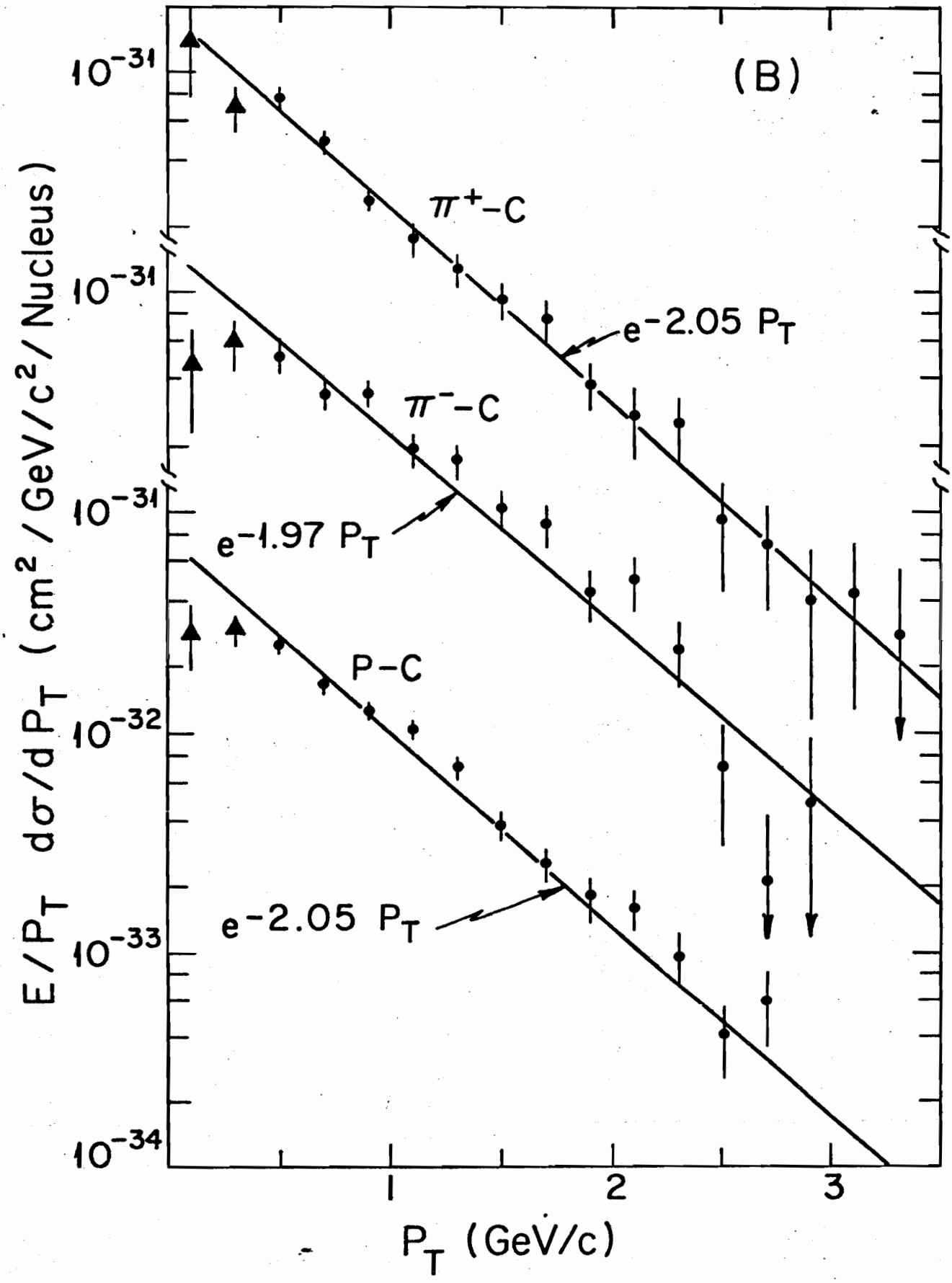
(B)
π^+-C
$e^{-2.05\ P_T}$
π^--C
$e^{-1.97\ P_T}$
P-C
$e^{-2.05\ P_T}$
10^{-31}
10^{-31}
10^{-31}
10^{-32}
10^{-33}
10^{-34}
$E/P_T\ d\sigma/d\,P_T$ (cm^2 / GeV/c^2/ Nucleus)
1
2
3
P_T (GeV/c)

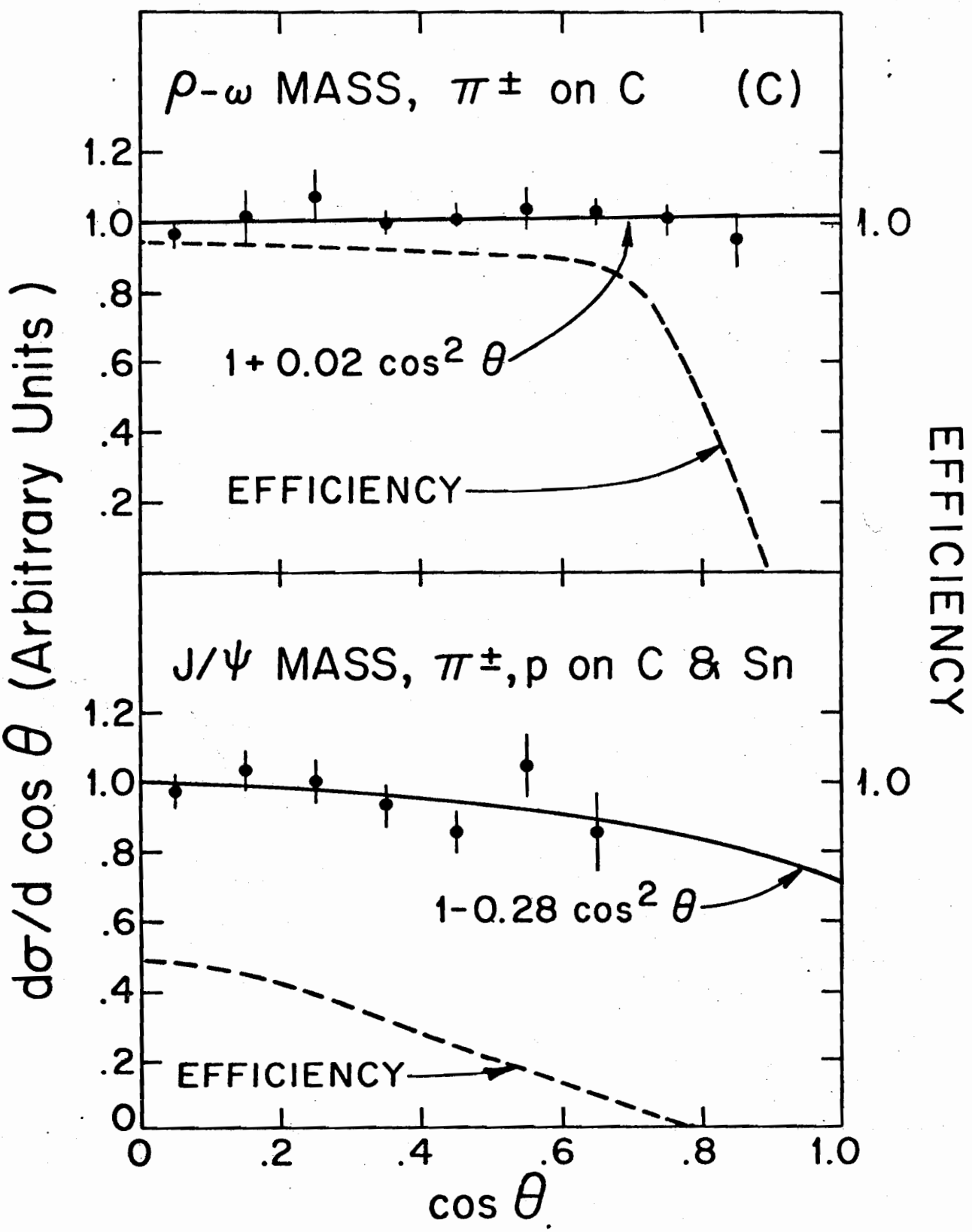
ρ-ω MASS, π± on C (C)
1.2
1.0
.8
.6
.4
.2
1+ 0.02 cos² θ
EFFICIENCY
1.0
EFFICIENCY
J/ψ MASS, π±, p on C & Sn
1.2
1.0
.8
.6
.4
.2
0
1-0.28 cos² θ
EFFICIENCY
1.0
dσ/d cos θ (Arbitrary Units)
0
.2
.4
.6
.8
1.0
cos θ

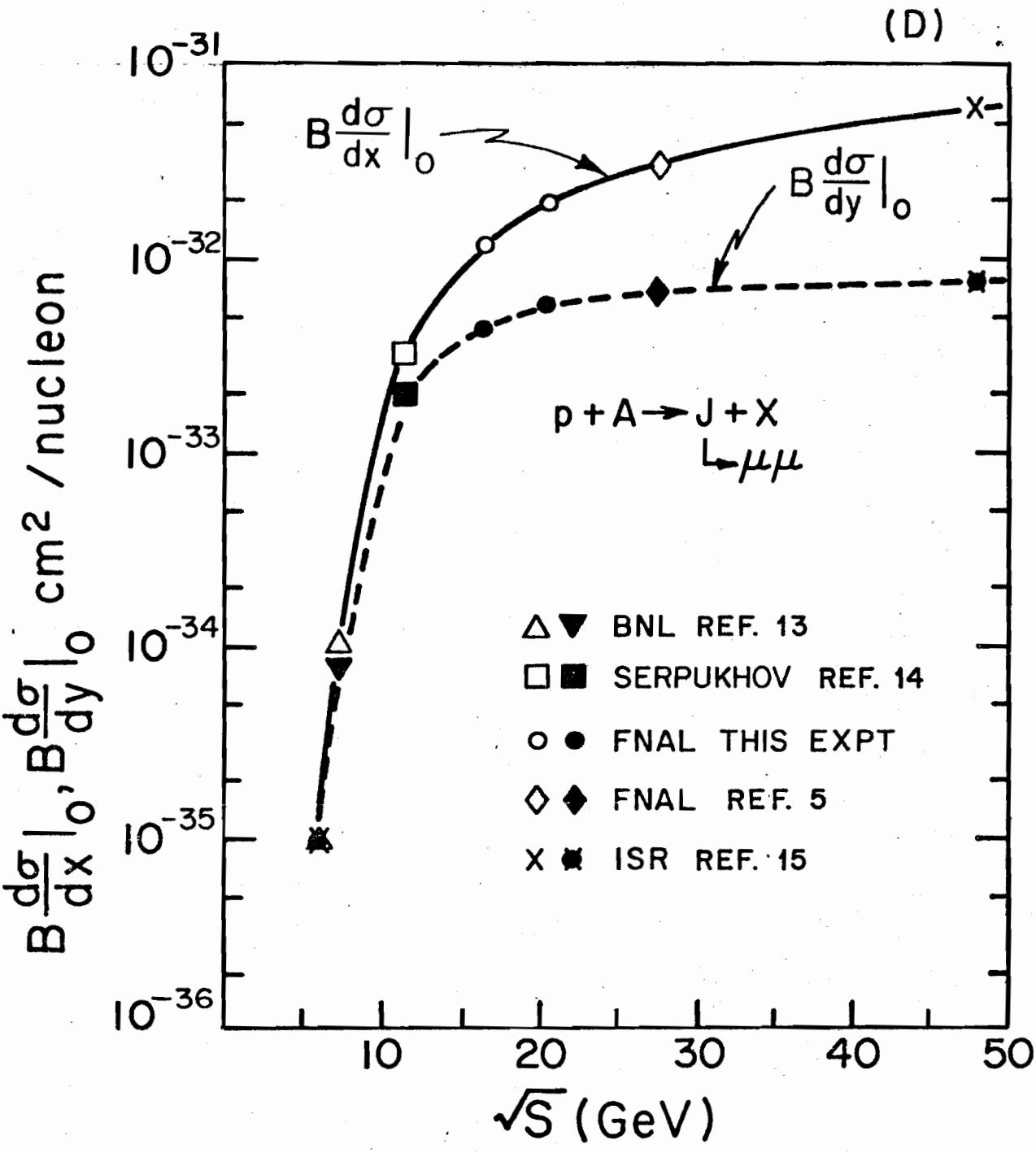
(D)
10^{-31}
10^{-32}
10^{-33}
10^{-34}
10^{-35}
10^{-36}
$B\frac{d\sigma}{dx}|_0$
$B\frac{d\sigma}{dy}|_0$
$B\frac{d\sigma}{dx}|_0, B\frac{d\sigma}{dy}|_0$ cm^2 / nucleon
p + A → J + X
↳ μμ
△▼ BNL REF. 13
□■ SERPUKHOV REF. 14
○● FNAL THIS EXPT
◇◆ FNAL REF. 5
X ✱ ISR REF. 15
10
20
30
40
50
$\sqrt{S}$ (GeV)